Quantum efficiency of stimulated emission in colloidal semiconductor nanocrystal quantum dots

Chunfeng Zhang, Jian Xu,* Ting Zhu, Fan Zhang, Zhanao Tan, and Steven J. Schiff
Department of Engineering Science and Mechanics, The Pennsylvania State University, University Park, Pennsylvania 16802, USA

Huaipeng Su and Shuai Gao
Department of Chemical Engineering, Tianjin University, Tianjin 300072, China

Andrew Y. Wang
Ocean NanoTech LLC., Fayetteville, Arkansas 72701-7175, USA

(Received 19 January 2009; revised manuscript received 17 June 2009; published 30 July 2009)

External differential quantum efficiencies were studied for the stimulated emission of thin films of colloidal CdSe/CdS/ZnS nanocrystal quantum dots (NQDs) using the integrating sphere technique. A maximum efficiency of 34% was measured for the stimulated emission in NQDs which far exceeds that for spontaneous emission (9%). The competition between the radiative exciton/biexciton recombination and the carrier density-dependent nonradiative relaxation processes in NQDs was modeled to account for the observed difference in efficiency.

DOI: 10.1103/PhysRevB.80.035333 PACS number(s): 78.67.Hc, 73.21.La

I. INTRODUCTION

Efficient and size tunable photoluminescence has long been observed in colloidal semiconductor nanocrystal quantum dots (NQDs), which renders them promising candidates for photonic devices such as light-emitting diodes and lasers.[1–3] The first observation of amplified spontaneous emission (ASE) in close-packed NQD films by Klimov *et al.*[1] spurred a broad spectrum of efforts to investigate the stimulated emission and lasing processes in NQDs in recent years. Coherent, stimulated emission from NQDs, spanning from blue to the near-infrared range of the spectrum,[4–13] has been realized with a variety of structures including slab waveguides, microrings, microspheres, photonic crystals, and distributed feedback resonators. These NQD-based coherent light sources hold great promise in information processing and lightwave communication, as well as bio/chemical sensing.

The photoluminescence emission from solutions of semiconductor NQDs has potential applications involving fluorescent labeling in the field of biological imaging. As a result, the quantum efficiency of this spontaneous emission has been widely studied. There has yet to be, however, any in-depth investigation focused on the quantum efficiency of the stimulated emission from NQD films. It is well known that the radiative exciton and biexciton recombination in many compound NQDs, including (Zn,Cd)(S,Se) and Pb(S,Se) nanocrystals, competes with the ultrafast Auger relaxation process. NQD samples of high-packing densities are thus favorable for producing sufficient optical gain.[1,5] Consequently, ASE and lasing have hitherto been observed mostly in NQD films of close-packed NQD solids[1] or in a high-filling NQD/matrix,[5] though they are also realizable by incorporating NQDs of lower densities in resonant microcavities of very high-quality factors.[14] The fluorescent (spontaneous) emission of many NQD films exhibit quantum yields (1–10 %) substantially lower than their solution counterparts (80–95 %) due to the less passivated surfaces of the dried nanocrystals. It is noteworthy, however, that these NQD films can still be efficient gain media for stimulated emission because the optical gain of NQDs is determined by the intrinsic Auger relaxation, that is, much faster than the nonradiative recombination via surface states.

In NQD films the wave-guiding effect greatly modifies the angular distribution of the emission, making the output pattern highly dependent on film compositions and structures. Therefore, an efficiency characterization of NQD film emission cannot be accomplished by simply comparing the light output intensity with that of a reference dye sample as in the fluorescence-quantum yield measurements of NQD solutions because this technique assumes an isotropic angular distribution of the fluorescent emission. A more suitable approach to characterize the emission efficiency of NQD films involves measurements using an integrating sphere. When a NQD film is placed inside an integrating sphere, the output emission of the film will be diffusely reflected by the barium sulfate-coated inner surface of the sphere and redistributed isotropically into the full range of solid angles. In this manner, the spectral and intensity detection of the light exiting from a small aperture in the sphere surface can be used for an accurate determination of the total number of photons emitted by the NQD film. The external differential quantum efficiency of NQD films, η_d, can then be calculated by its definition

$$\eta_d = \frac{\text{number of emission photons}}{\text{number of absorbed photons}}. \quad (1)$$

In this paper, we describe the experiment results of our integrating sphere characterization of the external differential quantum efficiency of CdSe/CdS/ZnS core-shell NQD films at room temperature. Efficiencies for both spontaneous and stimulated emission were studied over a wide range of optically excited NQD carrier densities, with the average number of photoexcited electron-hole pairs per nanocrystal achieved experimentally notated by $\langle N_{eh} \rangle$. A rapid rise in efficiency has been observed upon the transition from spontaneous to

stimulated emission in our NQD films, with a maximum value of 34% achieved with $\langle N_{eh} \rangle \sim 2.7$. The emission efficiency declined gradually upon further increasing the NQD excitation density. The competition between radiative exciton/biexciton recombination and the carrier density-dependent nonradiative recombination in NQDs was modeled to account for the observed variation in the external differential quantum efficiency. The model took into account the Poisson distribution of the photoexcited carriers as well as the unique, step-by-step Auger relaxation of the multiple electron-hole pairs in a quantum-confined system. The lifetimes of the radiative biexciton recombination and the Auger relaxation in NQDs were also determined by comparing the model with the measured decay of the stimulated emission. The resulting Auger lifetime agrees well with the reported values that were previously extracted using time-resolved absorption spectroscopy.

II. EXPERIMENTS

A. Sample preparation and characterization

The NQDs employed in the present study have core-shell structures consisting of CdSe crystalline cores and CdS/ZnS double shells, prepared using a synthetic route based on inorganic precursors and noncoordinating solvents.[15] The average size of the as-prepared core-shell nanocrystals is ~6 nm in diameter. Following a purification process, thin films of NQDs were spun cast from a toluene solution to form slab waveguides of ~500 nm nominal thickness on glass substrates. The packing density of the NQDs in the films was examined with cross-sectional TEM imaging, revealing a volume density of $\sim 4 \times 10^{18}$ cm^{-3} for core-shell NQDs in the waveguide structure. The measured refractive index of the NQD film was $n_{(NQD)} \sim 1.82$ at $\lambda = 633$ nm as compared to $n_{(glass)} \sim 1.45$ for the substrate.

B. Quantum efficiency measurement

For the efficiency measurement, the NQD films were placed inside an integrating sphere to facilitate collection and measurement of the highly divergent emission. The second harmonic of a Ti:sapphire femtosecond amplifier (800 nm, 1 kHz, 80 fs, Coherent Libra system) was introduced into the integrating sphere to optically excite the NQD film sample. The output of the integrating sphere was coupled to a 0.1 nm resolution SpectroPro spectrometer equipped with a silicon p-i-n photodetector. Both the dispersion of the spectrometer grating and the response of the photodetector were calibrated to ensure detection linearity. A barium sulfate-coated baffle was placed in front of the fiber coupler at the interior surface of the integrating sphere to prevent direct illumination of the optical fiber.

In the present study the external differential quantum efficiency, η_d, was measured following a three-step procedure,[16–18] as illustrated in Fig. 1(a). While an in-depth discussion of the measurement approach can be found elsewhere,[16] a brief description of our experiment procedure follows. In the first step (i), the excitation laser beam was introduced into the integrating sphere before the NQD

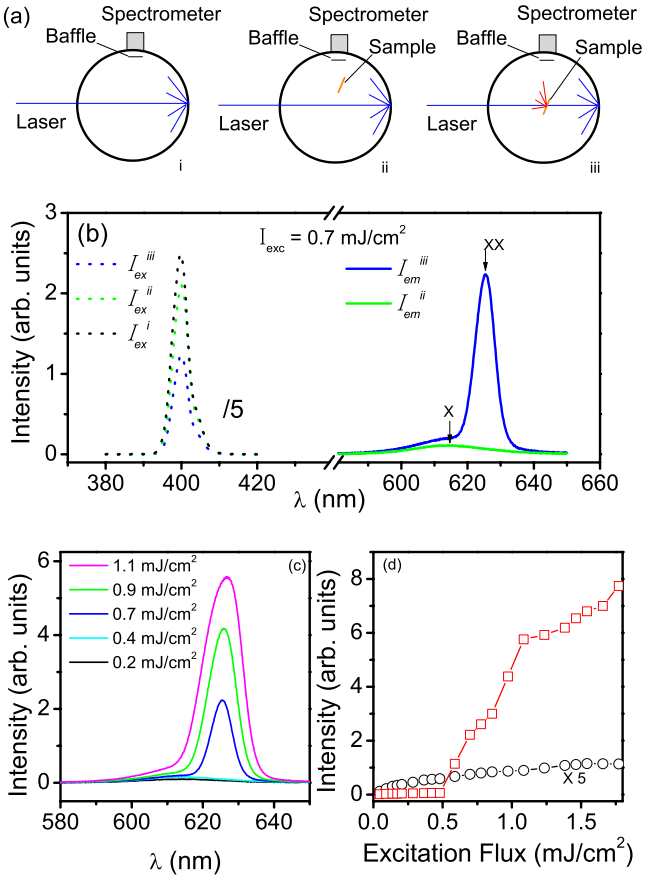

FIG. 1. (Color online) (a) Schematic diagram illustrating the three-step procedure for the integrating sphere measurement of the external differential quantum efficiency in NQDs; (b) spectra of scattered excitation light and emission from the NQD film under different pump fluence conditions with emission spectra primarily influenced by either single exciton (X) or biexciton (XX) recombination; (c) emission spectra recorded from step (iii) at different excitation fluences; (d) peak intensities of the stimulated emission (square) and spontaneous emission (circle) of NQDs versus the pump fluence.

sample was loaded, allowing for detection of the pump-laser light scattered by the interior surface of the sphere. The recorded output spectrum was normalized to the photon flux, as shown in Fig. 1(b). The excitation laser spectrum is centered at $\lambda = 400$ nm, with an integrated intensity, I_{ex}^{i}, that is, proportional to the pump-laser intensity. In the second step (ii), the sample was placed inside the sphere but was not under the direct excitation of the pump beam. Only a small fraction of the scattered pump-laser light was absorbed by the sample and hence a weak emission was recorded from the NQD sample. The photon-flux normalized output spectrum of this configuration is composed of two bands: the excitation band with an integrated intensity of I_{ex}^{ii} and the band of NQD emission with an integrated intensity of I_{em}^{iii}. In the third step (iii), the sample was irradiated by the pump beam directly. A portion of the pump light was absorbed upon initial propagation through the sample. In addition, a small fraction of the scattered residual light was reabsorbed by the sample as in step (ii). The photon-flux normalized

emission from the direct illumination configuration also includes two bands resulting in spectra from the excitation source, I_{ex}^{iii}, and the NQD emission, I_{em}^{iii}. The external differential quantum efficiency for the NQD film emission can then be calculated with the following equation,[16–18]

$$\eta_d = \frac{I_{ex}^{i} I_{em}^{iii} - I_{ex}^{ii} I_{em}^{ii}}{(I_{ex}^{i})^2 - I_{ex}^{i} I_{ex}^{ii}}. \quad (2)$$

In the integrating sphere, the NQD samples were photoexcited by focusing the pump beam to a ~1 mm spot on the surface of the NQD film. The pump fluence was varied between measurements to investigate the effect of the carrier density of NQD excitation on the external differential quantum efficiency and the aforementioned three-step procedure was repeated to extract the corresponding efficiency values.

III. RESULTS AND DISCUSSIONS

For a low pump fluence, the spontaneous emission of the NQD film peaks at $\lambda \sim 615$ nm with a full-width-at-half-maximum bandwidth of ~25 nm. When the pump fluence is increased to ~0.7 mJ/cm^2, the spectral profile of the NQD output exhibits a significant reduction in bandwidth, down to ~7 nm, which is characteristic of stimulated emission for the NQD film [Fig. 1(b)]. The peak of the stimulated emission spectra also exhibits a noticeable redshift of ~10 nm with respect to the spectral maximum from the spontaneous emission. The observed redshift has been interpreted as arising from the dominance of radiative biexciton recombination during stimulated emission as compared to the single-exciton process underlying the spontaneous emission in NQDs. Figures 1(c) and 1(d) show, respectively, the emission spectra recorded at step (iii) and the measured peak intensities for the single and biexciton emission of the NQD sample versus pump fluence. The noticeable threshold behavior for the biexciton emission at $J=0.5$ mJ/cm^2 adds further evidence to the primary role of the radiative recombination of biexcitons in the stimulation emission of CdSe/CdS/ZnS NQDs.

The presence of the biexcitons in CdSe-based NQDs arises from the twofold degeneracy of their ground electron states, which also predicts a carrier density of NQD excitation of $N_{eh} \sim 1$ for population inversion and, hence, the onset of the optical gain in NQDs.[1] In our experiment, the average carrier density of NQD excitation was determined by estimating the average number of photogenerated electron-hole pairs per nanocrystal, $\langle N_{eh} \rangle$, using the following relation

$$\langle N_{eh} \rangle = \frac{J \sigma_{\mathrm{NQD}}}{h \nu_{pump}}, \quad (3)$$

where J is the pump fluence, $h\nu_{pump}$ is the pump photon energy, and NQD is the measured absorption cross section of the CdSe/CdS/ZnS NQDs under study. The measured pump fluence for the onset of the stimulated emission in the NQD film, $J=0.5$ mJ/cm^2, corresponds to an average carrier density of $\langle N_{eh} \rangle = N^{TH} \sim 1.25$, where N_{TH} denotes the threshold carrier density. The greater value of N_{TH} as compared to the predicted carrier density for the onset of the optical gain ($\langle N_{eh} \rangle \sim 1$) is attributed to the internal losses in a NQD film, which often include light reabsorption and scattering in close-packed NQDs.[13]

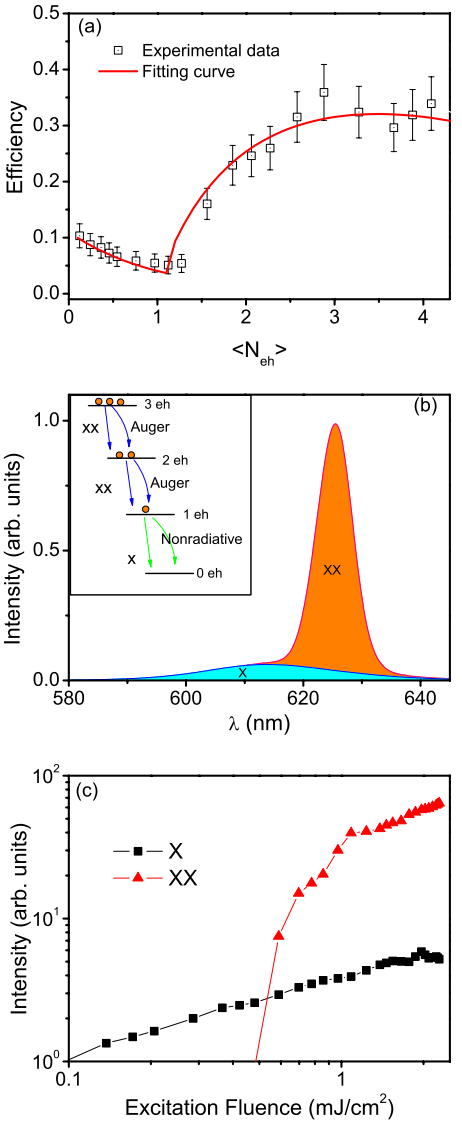

FIG. 2. (Color online) (a) External differential quantum efficiency of the emission of a NQD film plotted as a function of the average carrier density of NQD excitation. (b) Schematic diagram of the contributions of single exciton (X) and biexciton (XX) recombination in an amplified spontaneous emission spectrum. Inset shows the quantized steps of the Auger relaxation in NQDs. (c) Excitation fluence-dependent integrated intensity of single exciton emission (X) and biexciton emission (XX).

In order to investigate the radiation efficiency of NQDs, η_d has been calculated from the integrating sphere-measurement data using Eq. (2) and plotted as a function of $\langle N_{eh} \rangle$ in Fig. 2(a). A prominent feature of the η_d vs $\langle N_{eh} \rangle$ relation is the onset of a rapid rise in η_d at a threshold carrier density of $\langle N_{eh} \rangle = 1.25$, which leads to a maximum $\eta_d = 34\%$ at $\langle N_{eh} \rangle \sim 2.7$. Further increasing the carrier density of NQD excitation above $\langle N_{eh} \rangle = 2.70$, however, resulted in a slow reduction in η_d. At a low carrier density of NQD excitation the NQD emission is characterized by a low efficiency of $\eta_d = 9\%$ and drops further as $\langle N_{eh} \rangle$ is increased to N_{TH}.

In analyzing the results of our efficiency measurement, it is worth noting that the population distribution of photoexcited carriers is known to follow the Poisson distribution, where the probability of having m electron-hole pairs in a selected NQD is $e^{-\langle N_{eh}\rangle}\langle N_{eh}\rangle^m/m!$ $(m=1,2,\ldots)$ (Refs. 19 and 20) for an average initial carrier density per NQD of $\langle N_{eh}\rangle$. When the pump fluence is low, $\langle N_{eh}\rangle \ll N^{TH}$, the majority of the NQDs in the thin-film sample has either 0 or 1 photogenerated excitons following the Poisson distribution. The spontaneous emission of a NQD film is dominated by the radiative relaxation (RR) of single excitons, which competes primarily with the defect- and surface-state-mediated nonradiative recombination (NR) process as well as the slow ionization (SI) and fast ionization (FI) events in the close-packed NQDs. The recorded efficiency of $\eta_d \sim 9\%$ for the spontaneous emission of the NQD film is consistent in order of magnitude with the calculated radiation efficiency of single-exciton recombination, $\eta^{(1)}$, using the reported rates of NR $(R_{\mathrm{NR}} \sim 10^7\ \mathrm{s}^{-1})$, SI $(R_{\mathrm{SI}} \sim 10^5\ \mathrm{s}^{-1})$, FI $(R_{\mathrm{FI}} \sim 10^5 - 10^8\ \mathrm{s}^{-1})$, and RR of single-excitons $(R_{\mathrm{RR}}^{(1)} \sim 10^7\ \mathrm{s}^{-1})$,

$$\eta^{(1)} = \frac{R_{\mathrm{RR}}^{(1)}}{R_{\mathrm{RR}}^{(1)} + R_{\mathrm{NR}} + R_{\mathrm{SI}} + R_{\mathrm{FI}}}. \tag{4}$$

At high excitation intensities, the trap-filling effect could cause the variation in NQD photoluminescence efficiency. Nevertheless, the efficiency should then increase gradually with the excitation intensity until all the NQD traps get filled up (saturation). Such a speculation is in conflict with the observed threshold behavior in the experiment [Fig. 2(a)], allowing us to rule out the trap-filling effect in the present study. Furthermore, the observed coincident change in spectral profile [Fig. 1(c)] at the excitation threshold has suggested the key role of the biexciton gain. The emission spectrum of the NQD film can be deconvoluted into two overlapping spectral profiles that are associated with the radiative recombination of single excitons (X) and biexcitons (XX), respectively, as illustrated in Fig. 2(b). Figure 2(c) plots the integrated intensity of single exciton (X) and biexciton emission (XX) as the functions of exciton fluence, which suggests that the biexciton emission becomes more dominant when the excitation fluence rise beyond the threshold [Fig. 2(c)]. The $\langle N_{eh}\rangle$-dependent η_d can thus be interpreted by inspecting the intrinsic physical processes in the NQDs under different pumping conditions. When the average density of NQD excitation becomes significant and approaches N_{TH}, there is a continuously increasing population of NQDs containing two or more electron-hole pairs according to the Poisson distribution, which triggers quantum-confinement-enhanced Auger recombination in these nanoparticles. Since the multiple electron-hole pairs in a NQD can relax rapidly via the fast, nonradiative Auger recombination, they offer no contribution to the spontaneous emission before relaxing to the single-exciton state. Neither do they provide any optical gain in the NQD films due to the low density of biexcitons (Coulomb-correlated exciton pairs formed in the presence of two electron-hole pairs per NQD) at this pumping level. This leads to the observed decline in spontaneous emission efficiency as $<N_{eh}$ rises from 0 to N_{TH}, which can be modeled by assuming that only one electron-hole pair recombines radiatively in each of the NQDs initially containing multiple electron-hole pairs,

$$\eta_d = \frac{\Sigma \eta^{(1)} e^{-\langle N_{eh}\rangle}\langle N_{eh}\rangle^m/m!}{\langle N_{eh}\rangle} (0 < \langle N_{eh}\rangle < N^{TH}). \tag{5}$$

At an even higher pumping fluence the average carrier density of NQD excitation exceeds N^{TH} and the population of biexcitons in NQDs grows rapidly in accordance with the Poisson distribution. Since the radiative relaxation rate of biexcitons has been found to be several orders of magnitude larger than that of single excitons, the radiative recombination of biexcitons in NQDs can compete favorably with the nonradiative recombination events including fast Auger decay and, hence, results in optical gain and provides for the observed stimulated emission at a sufficiently large biexciton density in the NQD film. The radiation efficiency of the biexciton recombination, $\eta^{(2)}$, can be expressed as

$$\eta^{(2)} = \frac{R_{\mathrm{RR}}^{(2)}}{R_{\mathrm{RR}}^{(2)} + R_{\mathrm{AU}}^{(2)}}, \tag{6}$$

where $R_{\mathrm{RR}}^{(2)}$ is the radiative relaxation rate of biexcitons and $R_{\mathrm{AU}}^{(2)}$ is the Auger relaxation rate for two electron-hole pairs in a NQD. The fact that $R_{\mathrm{AU}}^{(2)}$ is several orders of magnitude higher than the rates of other nonradiative relaxation processes allows for disregarding R_{NR}, R_{SI}, and R_{FI} in the denominator of the above efficiency expression (6). For NQDs containing more than two electron-hole pairs, the carrier relaxation dynamics has been proposed by Klimov *et al.* to be a step-by-step process, e.g., from four pairs to three, and then to two pairs, with each step characterized by a discrete Auger rate, $R_{\mathrm{AU}}^{(m)}(m=3,4\ldots)$. The corresponding radiation efficiency for the relaxation of m electron-hole pairs in a NQD, $\eta^{(m)}$, can be modeled as

$$\eta^{(m)} = \frac{2}{m} \cdot \frac{R_{\mathrm{RR}}^{(2)}}{R_{\mathrm{RR}}^{(2)} + R_{\mathrm{AU}}^{(m)}} = \frac{2}{m(1 + m^2\xi^{(2)}/4)} (m = 2,3,\ldots), \tag{7}$$

where $\xi^{(2)} = R_{\mathrm{AU}}^{(2)}/R_{\mathrm{RR}}^{(2)}$ and the relation of $R_{\mathrm{AU}}^{(m)} = m^2 R_{\mathrm{AU}}^{(2)}/4$ has been used in deriving the efficiency expression.[20,21] The appearance of $R_{\mathrm{RR}}^{(2)}$ and $2/m$ in Eq. (7) originates from the fact that only two of the m electron-hole pairs in a NQD can occupy the ground biexciton state and thus contribute to the radiative path for the relaxation from m to m-1 electron-hole pairs in a nanoparticle [Fig. 2(b)].

Consequently, the external differential quantum efficiency of the NQD emission for $\langle N_{eh}\rangle > N^{TH}$ can be modeled, by taking into account both the single-exciton (spontaneous) emission and the biexciton (stimulated) emission as

$$\eta_d = \frac{\Sigma_{m\geq 1} \eta^{(1)} e^{-\langle N_{eh}\rangle}\langle N_{eh}\rangle^m/m!}{\langle N_{eh}\rangle} + \frac{\Sigma_{m\geq 2} \eta^{(m)} \Sigma_{k\geq m} e^{-\langle N_{eh}\rangle}\langle N_{eh}\rangle^k/k!}{\langle N_{eh}\rangle} - \frac{\Sigma_{m\geq 2} \eta^{(m)} \Sigma_{k\geq m} e^{-\langle N^{TH}\rangle}\langle N^{TH}\rangle^k/k!}{\langle N^{eh}\rangle}. \tag{8}$$

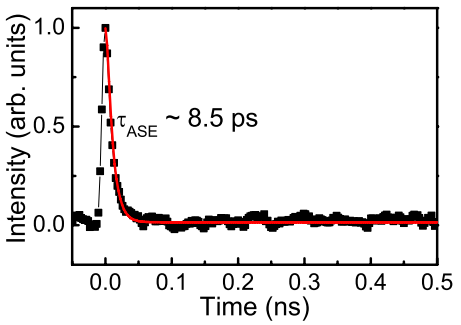

FIG. 3. (Color online) Time-resolved photoluminescence trace of the amplified spontaneous emission from the NQD film recorded at a pump fluence ~1 mJ/cm^2.

The first summation in Eq. (8) counts the efficiency for the spontaneous emission while the second summation models the efficiency for the stimulated emission due to the radiative relaxation of multiple electron-hole pairs in NQDs. A negative term has been introduced to the efficiency expression to represent the losses involved in the NQD film. The prevailing biexciton radiation in NQDs for $\langle N_{eh}\rangle > N^{TH}$ accounts for the rapid rise in η_d, as presented in Fig. 2(a), which is further confirmed by the observation of the redshifted biexciton emission peaks in Fig. 2(b). A close examination of Eqs. (7) and (8) suggests that η_d first increases with the carrier density of NQD excitation and then declines gradually after reaching a maximum value, as indicated in the efficiency plot [Fig. 2(a)]. Such a variation arises from the fact that $\eta^{(m)}$ decreases when $m>2$ as a consequence of the quadratic carrier-density dependence of the Auger rate. The overall efficiency of the stimulated emission therefore declines as a majority portion of the NQDs are photoexcited with more than two electron-hole pairs, which corresponds to an average carrier density of $\langle N_{eh}\rangle \sim 2.70$ in the experiment.

Finally, the measured values of the external differential quantum efficiency have been least-square fitted to Eqs. (5) and (8) in the proposed efficiency model by taking into account the high-order Auger relaxation up to $m=8$, which yielded a value of $\xi^{(2)}=R^{(2)}_{AU}/R^{(2)}_{RR}=0.14$. The deduced ratio between $R^{(2)}_{RR}$ and $R^{(2)}_{AU}$ makes it possible to determine the lifetimes of the Auger relaxation and the radiative recombination of biexcitons in NQDs if the lifetime of the stimulated emission is known. To facilitate this calculation, the Kerr gate technique has been employed to record the fast decay of the stimulated emission of the same NQD film.[22] The time-resolved photoluminescence trace of the amplified spontaneous emission from the NQD film is plotted in Fig. 3. A relaxation lifetime of $\tau=8.5$ ps was measured at the pump fluence corresponding to the maximum η_d, of $\langle N_{eh}\rangle=2.70$, which is about three orders faster than the spontaneous emission (~8 ns). The measured stimulated emission lifetime is an average value over all the NQDs

$$1/\tau = \frac{\Sigma_{m\geq 2} e^{-\langle N_{eh}\rangle}\langle N_{eh}\rangle^m (1/\tau^{(2)}_{RR} + 1/\tau^{(m)}_{AU})}{\Sigma_{m\geq 2} e^{-\langle N_{eh}\rangle}\langle N_{eh}\rangle^m/m!}, \quad (9)$$

where $\tau^2_{RR}=1/R^{(2)}_{RR}$ and $\tau^2_{AU}=1/R^{(2)}_{AU}$ are the lifetimes of the radiative recombination of biexcitons and the Auger relaxation in the NQDs with m electron-hole pairs, respectively. Solving Eq. (9) under the conditions of =8.5 ps and $\xi^{(2)}=R^{(2)}_{AU}/R^{(2)}_{RR}=0.14$ results in the determination of the respective lifetimes: $\tau^{(2)}_{RR}=13$ ps, $\tau^{(2)}_{AU}=89$ ps, $\tau^{(3)}_{RR}=40$ ps, and $\tau^{(4)}_{RR}=22$ ps. These Auger lifetimes agree well with the reported values that were previously extracted using time-resolved spectroscopy.[21,23,24] Also of note is our determination of the lifetime of the fast biexciton recombination in NQDs.

IV. CONCLUSION AND OUTLOOK

The uncovered efficiency of NQD emission here can be utilized to the future design of NQD emitters in a variety of applications. For instance, given the limitations of existing techniques[25–27] improving the rapid quantitative spatiotemporal measurement of small molecule metabolic analytes such as K^+ and O_2 within the nanoscale extracellular space of organs such as the brain would be very beneficial. The goals of fluorescent stability, ratiometric strategies to account for local concentration, ability to biological embed to protect cells and sensors, and extremely small size are all features which the NQD techniques of this paper can help serve in future work. It is also noteworthy that while the conclusions of the present study are valid for Cd(S,Se) NQDs II-VI compounds with high binding energy of exciton [on the order of 100 meV (Ref. 28)] and biexciton [on the order of 10 meV (Refs. 21, 29, and 30)],modifications to the model might be made in explaining the stimulated emission in NQDs of other compositions, such as PbS, PbSe, given the distinct difference in their energy-band structures.[7,31]

ACKNOWLEDGMENTS

The work at the Penn State University is being supported by the National Science Foundation under Grant No. CMMI-0729263 and Army Research Office under Grants No. 49653-EL and No. DURIP 2008-02-136, and that at Ocean NanoTech LLC is supported by the National Science Foundation under Grant No. 0638209.

*Corresponding author; jianxu@engr.psu.edu

[1] V. I. Klimov, A. A. Mikhailovsky, S. Xu, A. Malko, J. A. Holligsworth, C. A. Leatherdale, H. J. Eisler, and M. G. Bawendi, Science **290**, 314 (2000).

[2] J. M. Caruge, J. E. Halpert, V. Wood, V. Bulovic, and M. G. Bawendi, Nat. Photonics **2**, 247 (2008).

[3] P. O. Anikeeva, C. F. Madigan, J. E. Halpert, M. G. Bawendi, and V. Bulovic, Phys. Rev. B **78**, 085434 (2008).

[4] V. V. Sundar, H. J. Eisler, and M. G. Bawendi, Adv. Mater. (Weinheim, Ger.) **14**, 739 (2002).

[5] M. A. Petruska, A. V. Malko, P. M. Voyles, and V. I. Klimov, Adv. Mater. (Weinheim, Ger.) **15**, 610 (2003).
[6] H. J. Eisler, V. C. Sundar, M. G. Bawendi, M. Walsh, and H. I. Smith, Appl. Phys. Lett. **80**, 4614 (2002).
[7] R. D. Schaller, M. A. Petruska, and V. I. Klimov, J. Phys. Chem. B **107**, 13765 (2003).
[8] Y. Chan, J. S. Steckel, P. T. Snee, J. M. Caruge, J. M. Hodgkiss, D. G. Nocera, and M. G. Bawendi, Appl. Phys. Lett. **86**, 073102 (2005).
[9] A. V. Malko, A. A. Mikhailovsky, M. A. Petruska, J. A. Hollingsworth, H. Htoon, M. G. Bawendi, and V. I. Klimov, Appl. Phys. Lett. **81**, 1303 (2002).
[10] P. T. Snee, Y. Chan, D. G. Nocera, and M. G. Bawendi, Adv. Mater. (Weinheim, Ger.) **17**, 1131 (2005).
[11] V. C. Sundar, H. J. Eisler, T. Deng, Y. Chan, E. L. Thomas, and M. G. Bawendi, Adv. Mater. (Weinheim, Ger.) **16**, 2137 (2004).
[12] J.-Michel Caruge, Y. Chan, V. Sundar, H. J. Eisler, and M. G. Bawendi, Phys. Rev. B **70**, 085316 (2004).
[13] V. I. Klimov, S. A. Ivanov, J. Nanda, M. Achermann, I. Bezel, J. A. McGuire, and A. Piryatinski, Nature (London) **447**, 441 (2007).
[14] B. Min, S. Kim, K. Okamoto, L. Yang, A. Scherer, H. Atwater, and K. Vahala, Appl. Phys. Lett. **89**, 191124 (2006).
[15] Q. J. Sun, Y. A. Wang, L. S. Li, D. Y. Wang, T. Zhu, J. Xu, C. H. Yang, and Y. F. Li, Nat. Photonics **1**, 717 (2007).
[16] J. C. de Mello, H. F. Wittmann, and R. H. Friend, Adv. Mater. (Weinheim, Ger.) **9**, 230 (1997).
[17] Y. Zhang, R. E. Russo, and S. S. Mao, Appl. Phys. Lett. **87**, 043106 (2005).
[18] N. C. Greenham, I. D. W. Samuel, G. R. Hayes, R. T. Phillips, Y. A. R. R. Kessener, S. C. Moratti, A. B. Holmes, and R. H. Friend, Chem. Phys. Lett. **241**, 89 (1995).
[19] V. I. Klimov, J. Phys. Chem. B **104**, 6112 (2000).
[20] V. I. Klimov, A. A. Mikhailovsky, D. W. McBranch, C. A. Leatherdale, and M. G. Bawendi, Science **287**, 1011 (2000).
[21] V. Klimov, S. Hunsche, and H. Kurz, Phys. Rev. B **50**, 8110 (1994).
[22] C. F. Zhang, F. Zhang, S. E. Mohney, R. Henderson, and J. Xu, Opt. Lett. **33**, 2437 (2008).
[23] M. Califano, A. Franceschetti, and A. Zunger, Phys. Rev. B **75**, 115401 (2007).
[24] M. Achermann, J. A. Hollingsworth, and V. I. Klimov, Phys. Rev. B **68**, 245302 (2003).
[25] P. Padmawar, X. Yao, O. Bloch, G. T. Manley, and A. S. Verkman, Nat. Methods **2**, 825 (2005).
[26] H. Xu, J. W. Aylott, R. Kopelman, T. J. Miller, and M. A. Philbert, Anal. Chem. **73**, 4124 (2001).
[27] M. Brasuel, R. Kopelman, T. J. Miller, R. Tjalkens, and M. A. Philbert, Anal. Chem. **73**, 2221 (2001).
[28] R. W. Meulenberg, J. R. I. Lee, A. Wolcott, J. Z. Zhang, L. J. Terminello, and T. V. Buuren, ACS Nano **3**, 325 (2009).
[29] B. Patton, W. Langbein, and U. Woggon, Phys. Rev. B **68**, 125316 (2003).
[30] C. Burda, S. Link, T. C. Green, and M. A. El-Sayed, J. Phys. Chem. B **103**, 10775 (1999).
[31] V. Sukhovatkin, S. Musikhin, I. Gorelikov, S. Cauchi, L. Bakueva, E. Kumacheva, and E. H. Sargent, Opt. Lett. **30**, 171 (2005).